Incorporation of Drosophila CID/CENP-A and CENP-C into centromeres during early embryonic anaphase

Schuh, M; Lehner, C F; Heidmann, S

Incorporation of Drosophila CID/CENP-A and CENP-C into centromeres during early embryonic anaphase

Abstract

The centromere/kinetochore complex is indispensable for accurate segregation of chromosomes during cell divisions when it serves as the attachment site for spindle microtubules. Centromere identity in metazoans is believed to be governed by epigenetic mechanisms, because the highly repetitive centromeric DNA is neither sufficient nor required for specifying the assembly site of the kinetochore. A candidate for an epigenetic mark is the centromere-specific histone H3 variant CENP-A that replaces H3 in alternating blocks of chromatin exclusively in active centromeres. CENP-A acts as an initiator of kinetochore assembly, but the detailed dynamics of the deposition of metazoan CENP-A and of other constitutive kinetochore components are largely unknown. Here we show by quantitative fluorescence measurements in living early embryos that functional fluorescent fusion proteins of the Drosophila CENP-A and CENP-C homologs are rapidly incorporated into centromeres during anaphase. This incorporation is independent of ongoing DNA synthesis and pulling forces generated by the mitotic spindle, but strictly coupled to mitotic progression. Thus, our findings uncover a strikingly dynamic behavior of centromere components in anaphase.

Incorporation of *Drosophila* CID/CENP-A and CENP-C into centromeres during early embryonic anaphase

Melina Schuh*, Christian F. Lehner & Stefan Heidmann[§]

Bayreuth Center for Molecular Biosciences (BZMB), Department of Genetics, University of Bayreuth, 95440 Bayreuth, Germany

*Present address: European Molecular Biology Laboratory (EMBL), Gene Expression Unit, 69117 Heidelberg, Germany

[§]corresponding author

contact: stefan.heidmann@uni-bayreuth.de

Phone: ++49 921 55 58 14

Fax: ++49 921 55 27 10

Running head: Incorporation of CENP-A and CENP-C in anaphase

Summary

The centromere/kinetochore complex is indispensable for accurate segregation of chromosomes during cell divisions when it serves as the attachment site for spindle microtubules. Centromere identity in metazoans is believed to be governed by epigenetic mechanisms, as the highly repetitive centromeric DNA is neither sufficient nor required for specifying the assembly site of the kinetochore [1-4]. A candidate for an epigenetic mark is the centromere-specific histone H3 variant CENP-A that replaces H3 in alternating blocks of chromatin exclusively in active centromeres [1, 2, 5, 6]. CENP-A acts as an initiator of kinetochore assembly, but the detailed dynamics of the deposition of metazoan CENP-A and of other constitutive kinetochore components are largely unknown [1, 2, 7-10]. Here we show by quantitative fluorescence measurements in living early embryos that functional fluorescent fusion proteins of the *Drosophila* CENP-A and CENP-C homologs are rapidly incorporated into centromeres during anaphase. This incorporation is independent of ongoing DNA synthesis and pulling forces generated by the mitotic spindle, but strictly coupled to mitotic progression. Thus, our findings uncover a strikingly dynamic behavior of centromere components in anaphase.

Results and Discussion

We have analyzed the incorporation dynamics of the two constitutive centromere/kinetochore complex components described so far in *Drosophila*, the CENP-A homolog Centromere Identifier (CID) and the recently discovered, highly diverged CENP-C [11, 12]. CID and CENP-C were fused with the enhanced green fluorescent protein (EGFP) and enhanced yellow fluorescent protein (EYFP), respectively. The dynamics of the two fusion proteins were monitored during the syncytial nuclear divisions of the early *Drosophila* blastoderm embryo. These extremely rapid and synchronous cycles occur on the surface of the embryo allowing simultaneous data acquisition of multiple nuclei arranged in the same optical plane [13].

EGFP-CID and EYFP-CENP-C are specifically incorporated into centromeres during anaphase

We measured the cumulative centromere-localized fluorescence intensity of EGFP-CID and EYFP-CENP-C per nucleus throughout the cell cycle. While all sister centromeres are still grouped within one chromatin plate in metaphase, they are separated into two chromosome groups in anaphase. After the metaphase-to-anaphase transition, the fluorescence intensity per chromosome group is therefore expected to drop to 50% of the value observed in the metaphase plate. Subsequently, the fluorescence intensity is expected to increase to the initial value before the next mitosis, reflecting deposition of new EGFP-CID or EYFP-CENP-C. To reliably assign the cell cycle phase when this intensity increase occurs, we constructed strains co-expressing the green/yellow fluorescent centromere protein variants with a red fluorescent chromatin protein. For this purpose, we established a transgene expressing a functional histone 2A variant fused to the monomeric red

fluorescent protein [14] (His2Av-mRFP1). The expected sharp drop in fluorescence intensity was indeed recorded at anaphase onset, when the sister centromere groups of early anaphase figures were assigned to separate nuclei (Fig. 1A and C). Surprisingly, we detected immediately afterwards a steep increase in fluorescence intensity for both EGFP-CID and EYFP-CENP-C. This increase occurred during anaphase (Fig. 1A and C). The fluorescence increase during anaphase was also found for embryos expressing exclusively EGFP-CID in a *cid* mutant background (see Fig. S1), ruling out the possibility that the mitotic deposition of EGFP-CID is an artifact due to competition with endogenous, untagged CID. We point out that both EGFP-CID and EYFP-CENP-C are fully functional as they rescue the phenotypic consequences associated with *cid* and *Cenp-C* mutations, respectively (see Experimental Procedures and [11]). To exclude that the recorded intensity increase in anaphase results from a clustering of centromeres within the chromatin, we also analyzed the behavior of single centromeres (Fig. 1B, Supplementary Movie 1). Centromere fluorescence intensity was constant during interphase, but sharply dropped in late prophase/early metaphase, when individual sister centromeres are separated sufficiently by the pull of the mitotic spindle to allow their distinct quantification. During metaphase, the centromere fluorescence intensity stayed low. However, centromere fluorescence intensities strongly increased again during anaphase up to the level observed before sister centromere separation, thus confirming our quantification results of centromeric fluorescence per nucleus.

To assess whether the mitotic fluorescence intensity increase observed for centromeric chromatin components reflects a general behavior of chromatin proteins during the rapid syncytial divisions, we also monitored the fluorescence of His2Av-mRFP1. In this

case, a gradual increase throughout interphase was detected, while there was no substantial increase during mitosis (Fig. 1D). This pattern may indicate incorporation coupled with DNA replication which proceeds during the whole interphase in the syncytial cycles, or a continuous process involving replication-independent mechanisms recently described for the incorporation of His2A variants in *Drosophila* and budding yeast [15-18]. Regardless of the mechanism, bulk His2Av deposition during the syncytial divisions in *Drosophila* is clearly temporally distinct from incorporation of CENP-C or CID (Fig. 1D). To exclude that our quantification procedures artefactually generate a rapid signal increase during anaphase in case of point-like fluorescent signals, we analyzed a different fluorescent protein localized to a restricted chromosomal site. In these control experiments, we used a tetracyclin-repressor-EGFP fusion protein targeted to chromosomally integrated arrays of *tet*-operator repeats. No sharp increase in fluorescence intensity occurred during anaphase in this case (see Fig. S2).

EGFP-CID and EYFP-CENP-C are most dynamic during anaphase

To analyze the dynamics of EGFP-CID and EYFP-CENP-C during mitosis in more detail, we performed fluorescence recovery after photobleaching (FRAP) experiments. After bleaching of EGFP-CID signals with iterative pulses of the 488 nm laser at 100% power in metaphase, we observed a substantial recovery of fluorescence during anaphase (Fig. 2A, 58s and 139s; Supplementary Movie 2). For quantification, we bleached metaphase plates immediately before anaphase onset and measured the recovery of centromere-localized fluorescence of the bleached mitotic figures during anaphase. Significantly, in less than 2 min more than 100% of the initial fluorescence was recovered, which strongly supports incorporation of new EGFP-CID during anaphase. The analysis of FRAP in other cell cycle phases revealed that both EGFP-CID and EYFP-CENP-C are, by

at least a factor of 3, more dynamic during anaphase than during metaphase, telophase or interphase (Fig. S3).

Taken together, our results show that both CENP-C and CID are incorporated into centromeres during anaphase. Furthermore, as the fluorescence intensity after bleaching recovers within 2 min to values exceeding the values expected for exclusive new incorporation by approximately 30%, EGFP-CID exhibits also a surprising high turnover rate during anaphase. Recently, an increased turnover of all core histones during late mitosis has been observed in mammalian cells using FRAP analyses [19]. However, the recovery rates determined for the exchange of H3-GFP (approximately 15% recovery in 20 min) are much lower than the rates reported here for EGFP-CID. Thus the rapid exchange of EGFP-CID during anaphase likely is not due to a general higher histone exchange during late mitosis.

Anaphase incorporation of EGFP-CID and EYFP-CENP-C is independent of spindle microtubules but coupled to mitotic progression

The increased dynamics of EGFP-CID and EYFP-CENP-C observed during metaphase and anaphase is consistent with the idea that tension exerted by microtubules on the kinetochores permits the incorporation of new centromere/kinetochore complex components. Such an effect of tension on the incorporation of centromere identifying proteins would contribute to a faithful specification of centromere identity exclusively at functional centromeres [3]. To assess whether tension at the kinetochores is required for EGFP-CID and EYFP-CENP-C incorporation, we injected into syncytial embryos the

microtubule-destabilizing drug colcemid to abrogate tension, and then monitored the changes in fluorescence intensity. Since colcemid elicits the spindle checkpoint, which blocks cell cycle progression in wild type embryos before anaphase, we also injected embryos in which the spindle checkpoint was inactivated due to a mutation in the gene encoding the essential spindle assembly checkpoint kinase, Mps1 [20]. Progression through mitosis in these embryos took place despite the presence of colcemid as indicated by timely decondensation of the chromosomal DNA, which is a hallmark for late mitosis (Fig. 3A, *Mps1*$^{-/-}$, time point III). Interestingly, an increase in fluorescence intensity was recorded for both EGFP-CID (Fig. 3A, black curve) and EYFP-CENP-C (data not shown) before completion of chromosome decondensation. The fluorescence intensity of His2Av-mRFP1 did not change significantly during this period (Fig. S4A). These results show that both new EGFP-CID and EYFP-CENP-C are incorporated despite the absence of significant microtubule mediated tension at the kinetochore. When colcemid was injected into embryos with an intact spindle checkpoint, the nuclei entered mitosis and arrested with highly condensed chromosomes (Fig. 3A, bottom panel). However, no substantial net increase of EGFP-CID fluorescence above the initial value was observed, even over a period of about 14 min after entry into mitosis (Fig. 3A, red curve). Thus, the incorporation of the fluorescent centromere/kinetochore complex components is coupled to progression through mitosis.

Incorporation of EGFP-CID is independent of DNA replication

As DNA replication starts very early during the extremely rapid S-M cycles in syncytial *Drosophila* embryos, it is conceivable that the incorporation of the kinetochore

components takes place concomitant with and is dependent on, DNA synthesis. To test this assumption, we analyzed the dynamics of EGFP-CID after injection of syncytial embryos with the DNA synthesis inhibitor aphidicolin, which delays, but does not arrest, cell cycle progression at this stage [21, 22]. The injections were performed during late interphase to ensure that DNA synthesis is inhibited in the following cell cycle. The frequent occurrence of anaphase bridges in the mitosis immediately following the injection indicated that DNA synthesis was effectively inhibited already prior to mitosis in late replicating regions (Fig. 3B, bottom panel, arrowheads). Despite this inhibition, an increase in fluorescence intensity during anaphase to the initial value was observed (Fig. 3B). The fluorescence intensity of His2Av-mRFP1 did not change significantly during this period (Fig. S4B). These results suggest that incorporation of EGFP-CID during the syncytial divisions is completely uncoupled from DNA replication. Analyses of ectopically expressed proteins in HeLa and *Drosophila* Kc tissue culture cells [23, 24] as well as studies in *S. pombe* [25] have previously established that CID/CENP-A/Cnp1 incorporation can take place independently of DNA-replication. Furthermore, it has been shown in fission yeast and in human tissue culture cells that CENP-A homologs accumulate during late G2, well separated in time from DNA replication [24-26]. Since the syncytial nuclear cycles lack gap phases, we have also analyzed CID incorporation during the postblastoderm mitotic cycles 15 and 16, both of which have pronounced G2 phases. In these cases, EGFP-CID does not appear to become incorporated during anaphase (Fig. S5). Thus it appears that the mitotic incorporation of CID is a special feature of the rapid syncytial divisions occurring in the early *Drosophila* embryo and not a general mechanism.

The temporal separation of DNA synthesis and CID incorporation may prevent possible misincorporation into non-centromeric sites [8, 10, 12, 27, 28], which could lead to the fortuitous formation of ectopic kinetochores [8]. As a consequence of the delay between

DNA synthesis and CID loading, one might envision that either there are gaps in the nucleosomal array within centromeric chromatin that are filled in anaphase with CID nucleosomes or that during replication H3 is incorporated in centromeric chromatin, which then is replaced in anaphase by CID (Fig. 3C). Alternatively, CID is deposited in the immediate vicinity of centromeric chromatin saturated with CID-containing nucleosomes and serves as a reservoir for incorporation into new nucleosomes in the next cycle once the replication fork has passed the centromeric DNA and new nucleosomes are assembled (Fig. 3C).

Recently, it has been shown that in chicken DT-40 cells CENP-A incorporation is dependent (in part) on the presence of members of the CENP-H/CENP-I complex, which can be found at centromeres throughout the cell cycle [29]. While homologs for the vertebrate CENP-H/CENP-I complex components await their detection in *Drosophila*, in vitro assembly reactions have recently suggested a role of the chaperone RbAp48 in incorporation of CID into centromeric chromatin [30]. It has also been shown that CENP-A is mislocalized in the absence of the *S. pombe* RbAp48 homolog Mis16 or the human counterparts RbAp48 and RbAp46 [31]. It will be interesting to find out whether mitotic CID and CENP-C incorporation in syncytial *Drosophila* embryos is dependent on RbAp48. Also, as CID and CENP-C incorporation depends on mitotic progression, it might be coupled to the action of global cell cycle regulators like the anaphase-promoting complex/cyclosome, or kinases (Cdk1, Polo, Aurora) which are known to control progression through mitosis. Thus, these master regulators might also play a role in centromere propagation.

Conclusions

Our results show that new CID and CENP-C incorporation takes place during anaphase of the syncytial divisions of *Drosophila* embryos. This incorporation is independent of DNA replication and of normal pulling forces generated by the mitotic spindle. While it is counterintuitive that CID and CENP-C incorporation occurs while the centromeres are under strain by the pulling forces generated by the mitotic spindle, mitosis is the only time point in syncytial embryos without ongoing DNA synthesis. Thus, it appears that CID and CENP-C incorporation concomitant with DNA replication needs to be prevented. Our finding that CENP-C and CID incorporation during anaphase is independent of spindle pulling forces argues against the importance of tension in the epigenetic specification of the site of functional centromeres [3], at least for the syncytial divisions in *Drosophila* embryos. Nevertheless, as the mitotic spindle checkpoint enforces the dependence of anaphase on functional kinetochores, incorporation of centromere/kinetochore complex components only into functional kinetochores during anaphase may represent a safeguard mechanism to propagate centromeres.

Figure Legends

Fig. 1 *Drosophila* CID and CENP-C are incorporated into centromeres during anaphase. Living embryos expressing *EGFP-cid* (A, B) or *EYFP-Cenp-C* (C) together with *His2Av-mRFP1* or *His2Av-mRFP1* alone (D) were observed while progressing through mitosis 12. Fluorescence intensities of EGFP-CID (A), EYFP-CENP-C (C) and His2Av-mRFP1 (D) were determined for selected nuclei in each frame and are plotted as relative intensities per nucleus. Beginning at the onset of anaphase, segregating sister centromere groups or chromatin masses were evaluated separately, resulting in an approximately 50% intensity drop (labeled IV in (A) and I in (C) and (D)). Data sets from a total of 25 to 30 nuclei from three embryos were aligned. (B) EGFP-CID signal intensities of isolated single centromeres were evaluated and plotted per centromere. In this case, a 50% intensity drop occurs at the beginning of metaphase since the prominent poleward stretching of sister centromeres allowed a distinct evaluation of individual sister centromeres already at this stage. The subsequent fluorescence intensity increase during anaphase of individual centromeres is illustrated using a false color representation (B, insets in panels II and III, Look Up Table shown below). Images corresponding to selected time points (indicated by arrows numbered with roman numerals) of the series are displayed below the graphs. His2Av-mRFP1 is shown in red and EGFP-CID (A, B) and EYFP-CENP-C (C) in green. For comparison, the EGFP-CID graph (red) is superimposed on the His2Av-mRFP1 graph (black) in (D). Time points encompassing anaphase are indicated by the green rectangle in (D). Similar results were obtained when progression through mitosis 11 or mitosis 13 was monitored (data not shown). Gray lines in the graphs indicate the calculated fluorescence intensities of individual sister centromeres (B) or sister centromere groups per nucleus (A, C) or sister chromatids per nucleus (D) before their actual evaluation is possible. This renders the intensity increase during anaphase even more obvious. The values were

obtained by halving the measured intensities at the time points, when sister centromeres and chromatids are not yet sufficiently separated and therefore were not separately quantifiable. Data are presented as mean +/- SD.

Fig. 2 EGFP-CID is highly dynamic during anaphase. Living embryos expressing *His2Av-mRFP1* and *EGFP-cid* were observed while progressing through mitosis 12. Regions were selected (yellow oval in (A), first frame) and bleached. The recovery of centromeric EGFP-CID fluorescence was monitored. (A) Time lapse series after bleaching of a single metaphase plate. EGFP-CID is shown in green and His2Av-mRFP1 in red. (B) Quantitation of centromere-localized EGFP-fluorescence shows a recovery greater than 100% indicating net addition of new protein. The red arrow indicates the onset of anaphase. Data are presented as mean +/- SD.

Fig. 3 Abrogation of spindle-mediated tension and inhibition of DNA replication do not prevent EGFP-CID deposition. Living embryos expressing *His2Av-mRFP1* and *EGFP-cid* were observed while progressing through syncytial mitoses, and EGFP-CID fluorescence intensity was quantitated and plotted as in Fig. 1. Colcemid (A) or aphidicolin (B) were injected to inhibit spindle formation or DNA replication, respectively. The bottom panels show representative images of a single time lapse series for each experiment. EGFP-CID signals are shown in green and His2Av-mRFP1 signals in red. (A) Injected embryos were wild type ($Mps1^{+/+}$) or devoid of a functional spindle checkpoint due to the lack of the checkpoint kinase Mps1 ($Mps1^{-/-}$). Chromatin decondensation in (A, $Mps1^{-/-}$, frame III) indicates cell cycle progression in the absence of chromatid segregation, persistent

condensed chromosomes in (A, *Mps1*$^{+/+}$, frame 14 min) are due to a checkpoint arrest, and anaphase bridges (arrowheads in B) are indicative of incomplete replication during the preceding S-phase. Note the increase in EGFP-CID fluorescence during anaphase (B) or during DNA decondensation typical of late mitosis (A, *Mps1*$^{-/-}$). Such an increase is not present in checkpoint arrested nuclei (A, *Mps1*$^{+/+}$). The graphs represent average values obtained from 4 to 5 embryos. Data are presented as mean +/- SD. The gray line in B indicates the calculated fluorescence of sister centromeres before separation (see Fig. 1). (C) Models for CID incorporation temporally distinct from DNA replication. Color coded sectors indicate nucleosomal CID present prior to DNA replication (red), CID deposited during anaphase (green), centromeric associated CID incorporated during DNA replication (blue), or Histone H3 incorporated during DNA replication (yellow) (see text for details).

Supplemental data

Experimental Procedures, five supplemental figures and two movies are available with this article online.

Acknowledgements

We are indebted to Monika Willert-Porada and Ingrid Otto (Chair for Materials Processing, University of Bayreuth) for access to and help with the Zeiss LSM510 confocal system. We thank Katharina Trunzer, Oliver Schraidt, and Sebastian Götz for help with some experiments, the members of the lab for helpful discussions, and Jan Ellenberg for critical reading the manuscript. We are further thankful to Roger Tsien, Kim Nasmyth and Thom Kaufman for providing plasmids and *Drosophila* strains and to Björn Körtner for his help with writing PlugIns for ImageJ. This work was supported by a grant from the Deutsche Forschungsgemeinschaft (DFG He 2354/2-3)

References

1. Amor, D.J., Kalitsis, P., Sumer, H., and Choo, K.H. (2004). Building the centromere: from foundation proteins to 3D organization. Trends Cell Biol. *14*, 359-368.
2. Cleveland, D.W., Mao, Y., and Sullivan, K.F. (2003). Centromeres and kinetochores: from epigenetics to mitotic checkpoint signaling. Cell *112*, 407-421.
3. Mellone, B.G., and Allshire, R.C. (2003). Stretching it: putting the CEN(P-A) in centromere. Curr. Opin. Genet. Dev. *13*, 191-198.
4. Sullivan, B.A., Blower, M.D., and Karpen, G.H. (2001). Determining centromere identity: cyclical stories and forking paths. Nat. Rev. Genet *2*, 584-596.
5. Blower, M.D., Sullivan, B.A., and Karpen, G.H. (2002). Conserved organization of centromeric chromatin in flies and humans. Dev. Cell *2*, 319-330.
6. Carroll, C.W., and Straight, A.F. (2006). Centromere formation: from epigenetics to self-assembly. Trends Cell Biol. *16*, 70-78.
7. Fukagawa, T. (2004). Assembly of kinetochores in vertebrate cells. Exp. Cell Res. *296*, 21-27.
8. Heun, P., Erhardt, S., Blower, M.D., Weiss, S., Skora, A.D., and Karpen, G.H. (2006). Mislocalization of the Drosophila centromere-specific histone CID promotes formation of functional ectopic kinetochores. Dev. Cell *10*, 303-315.
9. Maddox, P.S., Oegema, K., Desai, A., and Cheeseman, I.M. (2004). "Holo"er than thou: chromosome segregation and kinetochore function in C. elegans. Chromosome Res. *12*, 641-653.
10. Van Hooser, A.A., Ouspenski, II, Gregson, H.C., Starr, D.A., Yen, T.J., Goldberg, M.L., Yokomori, K., Earnshaw, W.C., Sullivan, K.F., and Brinkley, B.R. (2001). Specification of kinetochore-forming chromatin by the histone H3 variant CENP-A. J. Cell Sci. *114*, 3529-3542.
11. Heeger, S., Leismann, O., Schittenhelm, R., Schraidt, O., Heidmann, S., and Lehner, C.F. (2005). Genetic interactions of separase regulatory subunits reveal the diverged Drosophila Cenp-C homolog. Genes Dev. *19*, 2041-2053.
12. Henikoff, S., Ahmad, K., Platero, J.S., and van Steensel, B. (2000). Heterochromatic deposition of centromeric histone H3-like proteins. Proc. Natl. Acad. Sci. USA *97*, 716-721.
13. Foe, V.E., and Alberts, B.M. (1983). Studies of nuclear and cytoplasmic behaviour during the five mitotic cycles that precede gastrulation in Drosophila embryogenesis. J. Cell Sci. *61*, 31-70.
14. Campbell, R.E., Tour, O., Palmer, A.E., Steinbach, P.A., Baird, G.S., Zacharias, D.A., and Tsien, R.Y. (2002). A monomeric red fluorescent protein. Proc. Natl. Acad. Sci. USA *99*, 7877-7882.
15. Kobor, M.S., Venkatasubrahmanyam, S., Meneghini, M.D., Gin, J.W., Jennings, J.L., Link, A.J., Madhani, H.D., and Rine, J. (2004). A protein complex containing the conserved Swi2/Snf2-related ATPase Swr1p deposits histone variant H2A.Z into euchromatin. PLoS Biol. *2*, E131.

16. Krogan, N.J., Baetz, K., Keogh, M.C., Datta, N., Sawa, C., Kwok, T.C., Thompson, N.J., Davey, M.G., Pootoolal, J., Hughes, T.R., et al. (2004). Regulation of chromosome stability by the histone H2A variant Htz1, the Swr1 chromatin remodeling complex, and the histone acetyltransferase NuA4. Proc. Natl. Acad. Sci. USA *101*, 13513-13518.
17. Kusch, T., Florens, L., Macdonald, W.H., Swanson, S.K., Glaser, R.L., Yates, J.R., 3rd, Abmayr, S.M., Washburn, M.P., and Workman, J.L. (2004). Acetylation by Tip60 is required for selective histone variant exchange at DNA lesions. Science *306*, 2084-2087.
18. Mizuguchi, G., Shen, X., Landry, J., Wu, W.H., Sen, S., and Wu, C. (2004). ATP-driven exchange of histone H2AZ variant catalyzed by SWR1 chromatin remodeling complex. Science *303*, 343-348.
19. Chen, D., Dundr, M., Wang, C., Leung, A., Lamond, A., Misteli, T., and Huang, S. (2005). Condensed mitotic chromatin is accessible to transcription factors and chromatin structural proteins. J. Cell Biol. *168*, 41-54.
20. Fischer, M.G., Heeger, S., Häcker, U., and Lehner, C.F. (2004). The mitotic arrest in response to hypoxia and of polar bodies during early embryogenesis requires Drosophila Mps1. Curr. Biol. *14*, 2019-2024.
21. Raff, J.W., and Glover, D.M. (1988). Nuclear and cytoplasmic mitotic cycles continue in *Drosophila* embryos in which DNA synthesis in inhibited with Aphidicolin. J. Cell Biol. *107*, 2009-2017.
22. Sibon, O.C.M., Stevenson, V.A., and Theurkauf, W.E. (1997). DNA-replication checkpoint control at the Drosophila midblastula transition. Nature *388*, 93-97.
23. Ahmad, K., and Henikoff, S. (2001). Centromeres are specialized replication domains in heterochromatin. J. Cell Biol. *153*, 101-110.
24. Shelby, R.D., Monier, K., and Sullivan, K.F. (2000). Chromatin assembly at kinetochores is uncoupled from DNA replication. J. Cell Biol. *151*, 1113-1118.
25. Takahashi, K., Takayama, Y., Masuda, F., Kobayashi, Y., and Saitoh, S. (2005). Two distinct pathways responsible for the loading of CENP-A to centromeres in the fission yeast cell cycle. Philos. Trans. R. Soc. Lond. B. Biol. Sci *360*, 595-607.
26. Shelby, R.D., Vafa, O., and Sullivan, K.F. (1997). Assembly of CENP-A into centromeric chromatin requires a cooperative array of nucleosomal DNA contact sites. J. Cell Biol. *136*, 501-513.
27. Ahmad, K., and Henikoff, S. (2002). Histone H3 variants specify modes of chromatin assembly. Proc. Natl. Acad. Sci. USA *99 Suppl 4*, 16477-16484.
28. Sullivan, K.F., Hechenberger, M., and Masri, K. (1994). Human CENP-A contains a histone H3 related histone fold domain that is required for targeting to the centromere. J. Cell Biol. *127*, 581-592.
29. Okada, M., Cheeseman, I.M., Hori, T., Okawa, K., McLeod, I.X., Yates, J.R., 3rd, Desai, A., and Fukagawa, T. (2006). The CENP-H-I complex is required for the efficient incorporation of newly synthesized CENP-A into centromeres. Nat. Cell Biol. *8*, 446-457.
30. Furuyama, T., Dalal, Y., and Henikoff, S. (2006). Chaperone-mediated assembly of centromeric chromatin in vitro. Proc. Natl. Acad. Sci. USA *103*, 6172-6177.

31. Hayashi, T., Fujita, Y., Iwasaki, O., Adachi, Y., Takahashi, K., and Yanagida, M. (2004). Mis16 and Mis18 are required for CENP-A loading and histone deacetylation at centromeres. Cell *118*, 715-729.

Schuh et al, Figure 1

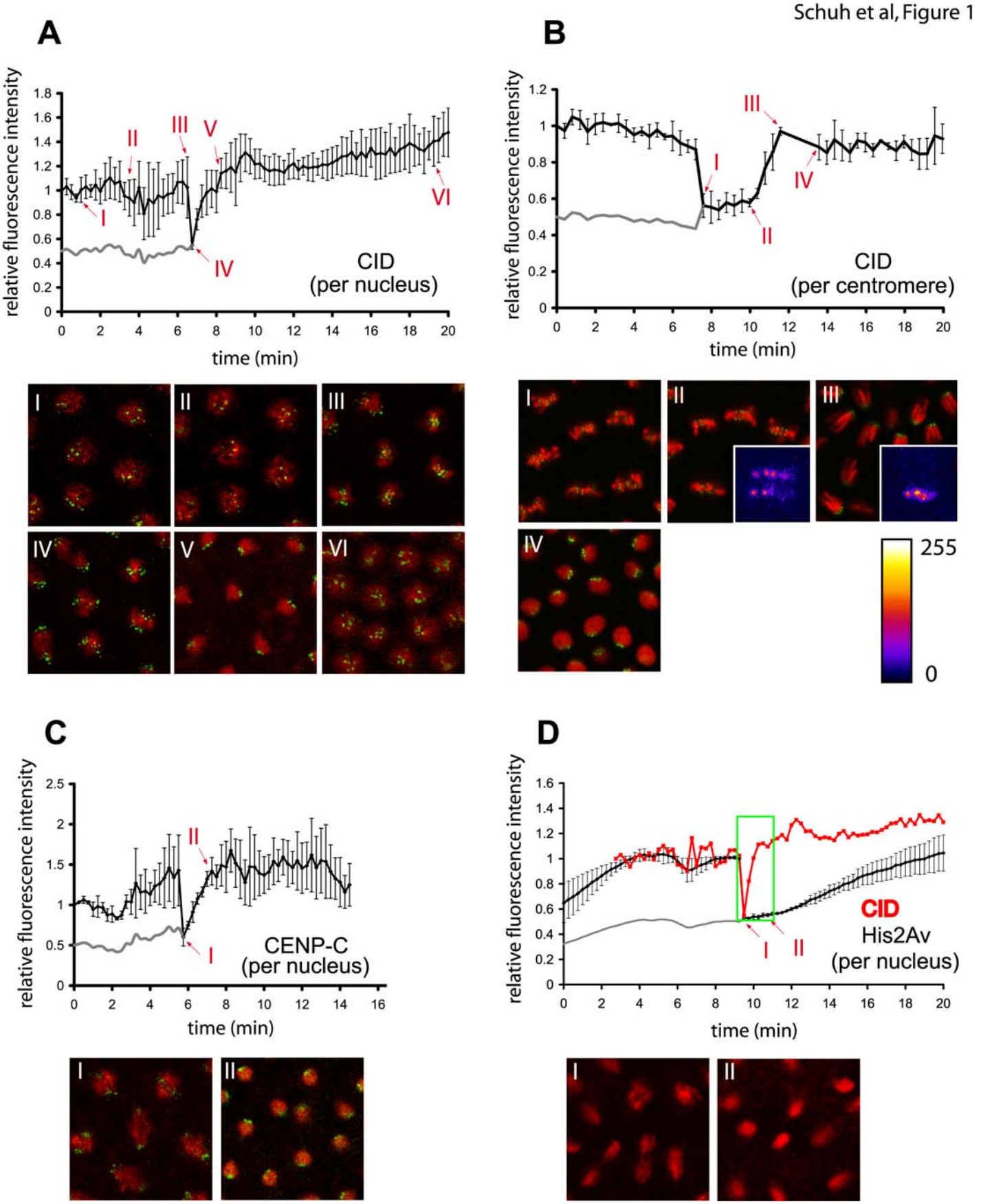

A

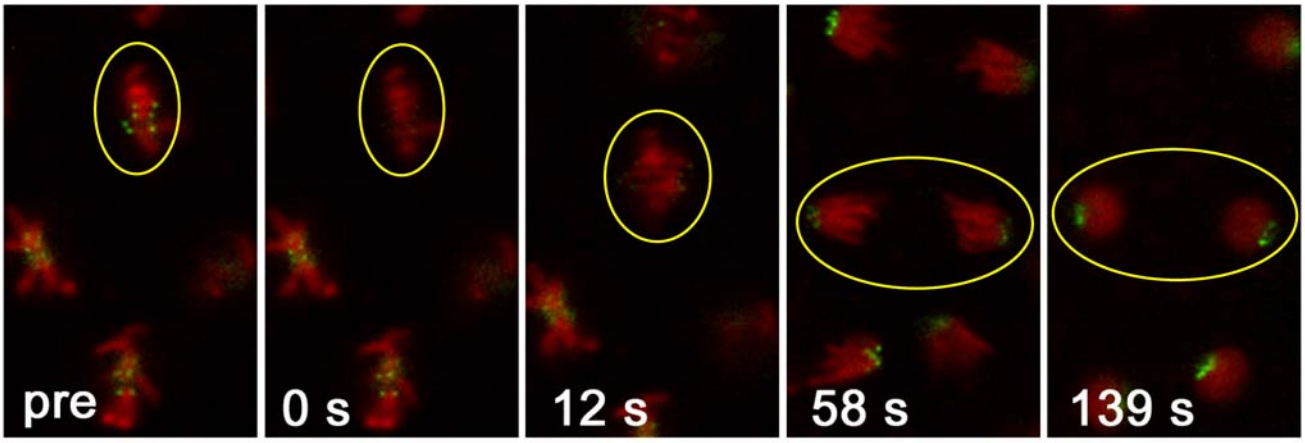
pre
0 s
12 s
58 s
139 s

B

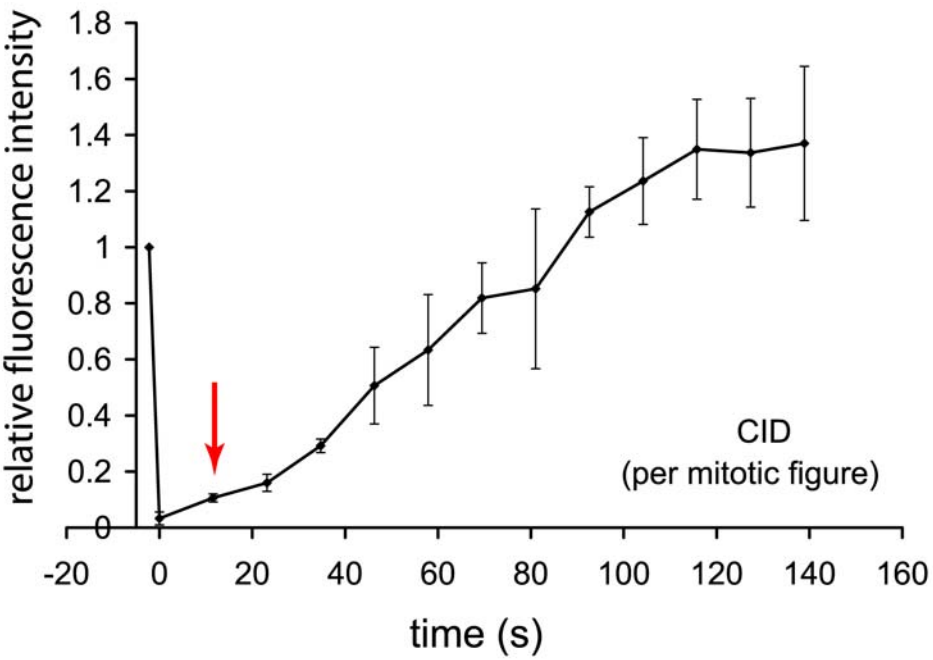
relative fluorescence intensity
1.8
1.6
1.4
1.2
1
0.8
0.6
0.4
0.2
0
-20
0
20
40
60
80
100
120
140
160
time (s)
CID
(per mitotic figure)

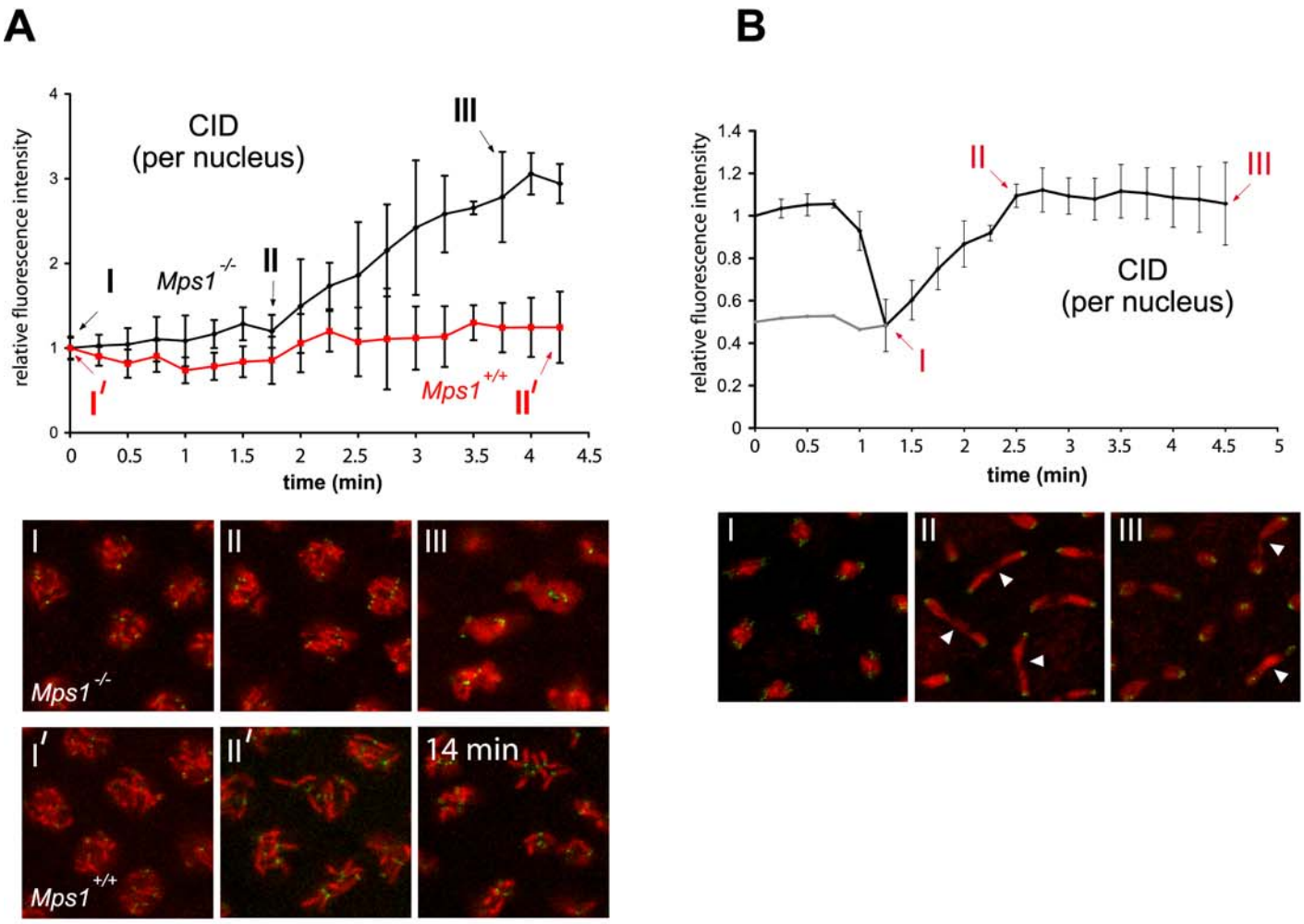
A
CID
(per nucleus)
relative fluorescence intensity
time (min)
Mps1 -/-
Mps1 +/+
I
II
III
I′
II′
B
CID
(per nucleus)
relative fluorescence intensity
time (min)
14 min

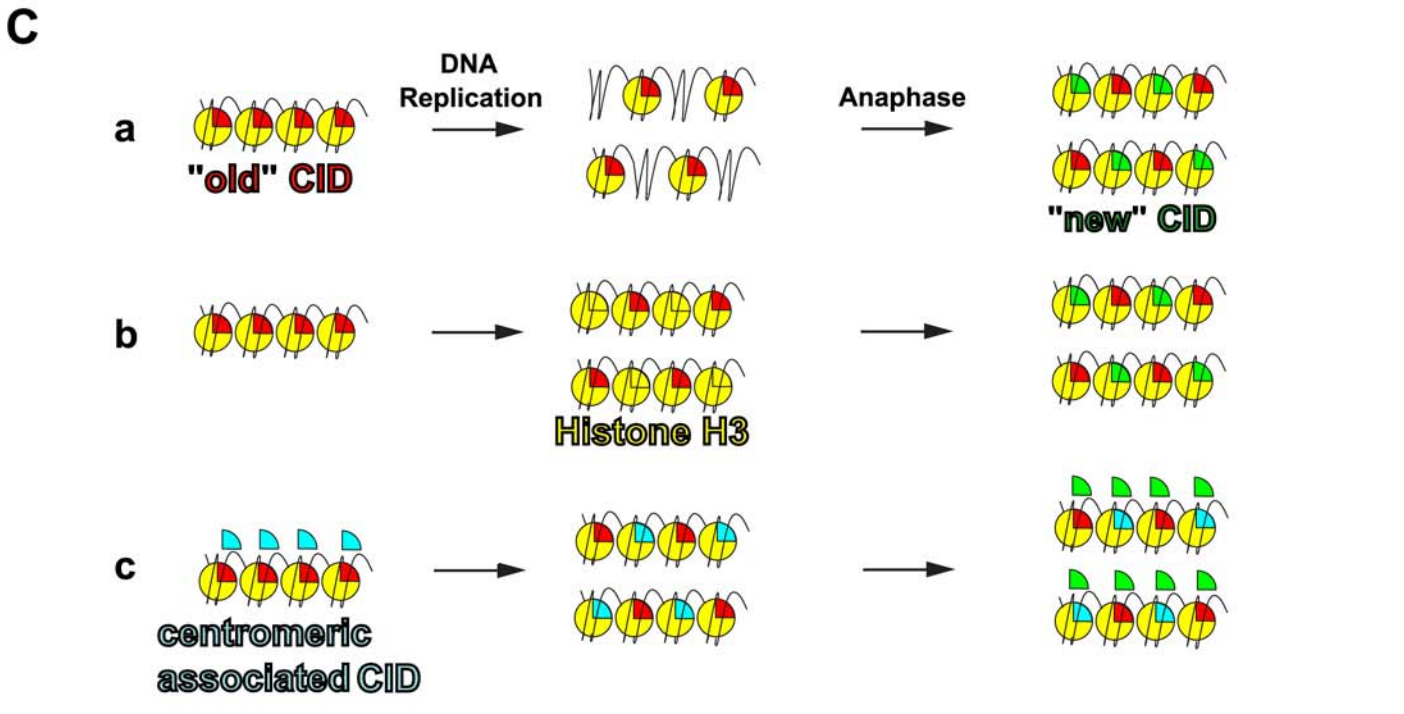
C
a
"old" CID
DNA
Replication
Anaphase
"new" CID
b
Histone H3
c
centromeric
associated CID

Supporting online material

Experimental Procedures

DNA constructs

For the construction of a green fluorescent CID variant, the EGFP coding sequence was inserted into an internal position for the following reasons. Our previous studies have indicated that a C-terminally tagged CID variant is only partially functional. The fusion protein localizes to the centromere, but the corresponding transgene fails to complement the lethality associated with *cid* mutants (unpublished observation). Similar observations were described for a C-terminally fused mouse CENP-A-GFP construct [S1]. Moreover, the N-terminus of CID is thought to be required for the recruitment of other kinetochore components. Thus, we left the free N-terminus unscathed and inserted the EGFP coding region within the CID N-terminal tail (between the codons specifying amino acids 118 and 119), directly upstream of an 11 amino acid stretch which is conserved among various Drosophilids and which in all cases immediately abuts the histone fold domain [S2]. First, a 772 bp fragment encompassing 412 bp upstream of the *cid* translational initiation codon and 354 bp of the coding region up to codon 118 was PCR-amplified using w^1 genomic DNA as template, the oligodeoxynucleotides DW4 (5'-CGG **GGTACC** CGACATGGCTGTATCTTCAG -3') and DW10 (5'-CGC **GGATCC** GGTCTGGTTTTGCGCAGCA -3'), and the Long Range PCR amplification kit (Roche Biochemicals) according to the manufacturer's recommendations. A second fragment encompassing the EGFP coding region was amplified using *Pfu*-Polymerase, the plasmid pBac{3xP3-EGFPaf} [S3] as template and the oligodeoxynucleotides DW6 (5'- CGC **GGATCC** GGCGGCGGCATGGTGAGCAAGGGCGAG-3') and DW7 (5'-CCAC **AAGCTT** GCCGCCGCCCTTGTACAGCTCGTCCATGC -3'). These

oligodeoxynucleotides introduced restriction sites as well as three codons for glycine residues at both sides of EGFP to serve as flexible linker. The two PCR fragments were cleaved at the restriction sites introduced by the primers (shown in bold type) and cloned simultaneously into pBluescript (Stratagene). A third fragment encompassing the *cid* region coding for amino acids 119 through 225 as well as 513 bp of the flanking 3'-genomic region was PCR-amplified using w^1 genomic DNA as template, the oligodeoxynucleotides DW11 (5'- CCAC **AAGCTT** AGGCGGCGCAAAGCGGC-3') and DW3 (5'- CTAG **TCTAGA** GGTGACTCATTTCAAAAAGCG-3') and cloned simultaneously with the 5'-*cid-EGFP*-fused fragment isolated from the pBluescript clone into the transformation vector pCaSpeR4 [S4].

To obtain lines expressing the fly histone H2 variant His2Av fused to mRFP1 [S5], a construct very similar to that used by Clarkson and Saint [S6] for the expression of His2Av-GFP was assembled in Litmus 28 (New England Biolabs). First, a 2240 bp fragment encompassing 751 bp upstream of the His2Av translational initiation codon and the complete His2Av coding region up to the ultimate codon was PCR-amplified using w^1 genomic DNA as template, the oligodeoxynucleotides SH141 (5'-GGT **TCTAGA** TCTCACCGAATCCTCC-3') and SH142 (5'-GGTC **ACCGGT** CCGTAGGCCTGCGACAGAATG-3'), and the Long Range PCR amplification kit. This fragment was cut with *Age*I and *Xba*I and cloned into an equally cleaved Litmus 28. The mRFP1 coding region was amplified using the oligodeoxynucleotides SH146 (5'-GGTA **ACCGGT** CGATAAGGATCCGATGG-3') and SH147 (5'-GCAGCCGGATC **AAGCTT** CG-3') and pRSETB-mRFP1 (gift of Roger Tsien, San Diego) as template, and the resulting fragment was cloned in frame as an *Age*I/*Hin*dIII fragment downstream of the His2Av coding region. A 1690 bp fragment of genomic His2Av 3'-flanking DNA was amplified using the

oligodeoxynucleotides SH143 (5'-GGA **AAGCTT** AAGCCAGTCGGCAATCGG-3') and SH144 (5'-GGA **ACTAGT** AAGATCTGCTGGATGAGGAC-3') and w^1 genomic DNA as template, and was cloned downstream of the *His2Av-mRFP1*-fusion as a *Hin*dIII/*Spe*I fragment. The integrity of PCR-amplified protein coding regions was verified by DNA sequencing. The final assembled construct was excised as a 4630 bp *Bgl*II fragment and cloned into a *Bam*HI cleaved transformation vector pCaSpeR4.

Strains allowing maternal expression of the *NLS-tetR-EGFP* fusion gene under control of the *nanos* (*nos*) promoter and with the *α1-tubulin* (*α1tub*) 3'-UTR were constructed as follows. First, the EGFP coding region was obtained as a *Bam*HI/*Hin*dIII fragment from pCaSpeR4-EGFP-cid and cloned into Litmus28. Then, the *tetR* coding region including an N-terminal fused nuclear localization signal (NLS) was PCR-amplified using as template the plasmid p128tetR-GFP, which had been shown to direct expression of *NLS-tetR-GFP* in yeast cells [S7]. The PCR product was cloned in frame upstream of EGFP in Litmus28-EGFP. A 917 bp genomic fragment containing the 5'-UTR and upstream regulatory sequences of the *nos* gene as well as an 860 bp genomic fragment containing the 3'UTR and downstream flanking sequences of the *α1tub* gene were PCR-amplified using the Long Range PCR amplification kit and w^1 genomic DNA as template. These two regions have been shown to direct maternal expression of transgenes throughout the early Drosophila embryo [S8]. The *nos* 5'and *α1tub* 3' PCR fragments were then cloned successively upstream and downstream of NLS-tetR-EGFP, respectively. PCR-amplified coding regions were verified by DNA sequence analysis. The final assembled construct was excised as a 3189 bp *Spe*I/*Asp*718 fragment and cloned into pCaSpeR4. 224 tandem copies of the *tet*-operator sequence were obtained as an 11.5 kb *Bam*HI/*Bgl*II fragment from the plasmid p306tetO224 [S7] and were also cloned into pCaSpeR4.

Fly strains

Transgenic *Drosophila* lines were obtained after P-element-mediated germ line transformation following standard procedures. Both *His2Av-mRFP1* and *EGFP-cid* were expressed under control of the respective genomic regulatory sequences. To assay whether the *EGFP-cid* transgene is functional, complementation assays were performed with the lethal null mutant alleles $cid^{T12\text{-}1}$ and $cid^{T22\text{-}4}$ [S9]. When provided by the mother, a single copy of the transgene insertion *EGFP-cid* III.2 complements the lethality associated with the transheterozygous *cid* null mutant situation $cid^{T12\text{-}1}/cid^{T22\text{-}4}$ with high efficiency (88% of expected; 1224 progeny scored). A rescue stock expressing exclusively *EGFP-cid* could be established with two copies of the *EGFP-cid* III.2 transgene insertion. The *His2Av-mRFP1* transgene is also functional as it complements the lethality associated with the hemizygous *His2Av* mutant situation $His2Av^{05146}$/*Df(3R)ro80b* (data not shown).

Strains expressing EYFP fused to Drosophila CENP-C (EYFP-CENP-C) [S10], the $Mps1^{1}$ allele [S11], as well as the generation of $Mps1^{1}$ germ line clones to obtain eggs without maternal $Mps1^{+}$ contribution have been described previously [S11]. Strains expressing *His2Av-mRFP1* together with *EGFP-cid* or *EYFP-Cenp-C* in an $Mps1^{1}$ heterozygous mutant background appropriate for germ line clone production were constructed using standard genetic techniques. *His2Av* and *cid* mutant strains to test the biological functionality of the transgenes were obtained from the Bloomington *Drosophila* stock center or were kindly provided by Thom Kaufman, respectively.

Among the *tetop* transgenic lines, a double insertion on the third chromosome (line *tetop* III.1/*TM3, Ser*) allowed observation of GFP dots in living syncytial embryos with the best signal to noise ratio.

In vivo imaging

Embryos expressing *His2Av-mRFP1* alone or in combination with *EGFP-cid* or *EYFP-Cenp-C* were obtained and prepared as described previously [S12]. After ageing to the appropriate stage under halocarbon oil, embryos were observed while progressing through epidermal mitoses 10-13. Non-saturated images were acquired every 15 s with an inverted Leica DM-IRBE/TCS SP1 confocal system equipped with a 40x/1.25 oil immersion objective. For the FRAP experiments and the evaluation of single centromeres, an upright Zeiss LSM510 confocal system equipped with a 63x/1.40 oil immersion objective was used. Both confocal systems were equipped with 488 nm Ar lasers and 543 nm He/Ne lasers for the excitation of EYFP/EGFP and mRFP1, respectively. To allow for gas exchange when using the upright Zeiss microscope, we placed the immobilized embryos in a halocarbon oil filled chamber sealed at the bottom with a gas permeable membrane (YSI). For the FRAP analyses, a region of interest (R.O.I.) was selected and the centromeric signals were bleached with four (Fig. 2) or eight (Fig. S3) pulses of the argon laser at 100% power. Images were acquired every 11.5 sec (Fig. 2) or every 3.9 sec (Fig. S3) after bleaching.

Quantitation of in vivo imaging data

Quantitation of pixel intensities was performed using the software ImageJ (ver. 1.34n) (http://rsb.info.nih.gov/ij/index.html). For the determination of EGFP-CID and EYFP-CENP-C fluorescence intensities as shown in Figs. 1A, 1C, and 3B, nuclear regions were identified in the red (chromatin) channel by a segmentation algorithm (Gaussian and anisotropic diffusion filtering [S13] followed by application of an appropriate threshold). These regions were used as R.O.I.s to determine the mean pixel intensities and area of the accordingly segmented EGFP-CID or EYFP-CENP-C signals in the green channel per nucleus using the original unfiltered images. For background correction, cytoplasmic regions outside the

chromatin areas were identified by segmentation, and the mean cytoplasmic pixel intensities in the green channel were subtracted from the mean centromeric pixel intensities. The absolute centromeric fluorescence intensities per nucleus were calculated by multiplying the background corrected mean centromeric pixel intensities with the number of evaluated pixels within the individual R.O.I.s. In cases where the segmentation algorithm did not accurately assign R.O.I.s for the individual centromere groups (particularly during prophase and early anaphase), R.O.I.s were selected manually. For every time point in each experiment, the 10 or 5 (in case of one EYFP-CENP-C time series) highest values of corrected nuclear centromeric fluorescence intensity were selected and used to calculate a mean value per nucleus for this time point. The mean values per nucleus from three time series were aligned using the metaphase-to-anaphase transition as reference point, normalized to the first displayed time point in interphase, and mean values for the three series were calculated and plotted. The fluorescence intensities for His2Av-mRFP1 (Fig. 1D and Fig. S4) were determined in the red channel accordingly.

For the determination of EGFP-CID and EYFP-CENP-C fluorescence intensities after injection of colcemid as shown in Fig. 3A, R.O.I.s were selected manually and the background correction was performed as described above. As the nuclei in colcemid injected embryos do not segregate their DNA, the onset of chromosome condensation was used to align the data sets obtained from different embryos (four sets for *Mps1*$^{-/-}$ embryos and five sets for *Mps1*$^{+/+}$ embryos). While the centromeres are grouped in interphase at the apical surface of the nuclei, they redistribute rapidly throughout the nuclear space when the nuclei enter mitosis. Thus, our analysis of fluorescence intensities during the early stages of mitosis using single confocal planes did not permit the simultaneous evaluation of all centromere signals in the selected nuclei, resulting in a decrease of the measured intensities. This effect is exacerbated when no microtubules are present. As the first data points displayed in Fig. 3A

were taken from nuclei in early mitosis, the actual measured fluorescence intensity is lower than during the preceding interphase. Thus, the EGFP-CID fluorescence intensities for the *Mps1*$^{-/-}$ nuclei increase after progression through mitosis to values greater than twice the initial value displayed in the graph.

For the FRAP analyses (Figs. 2 and S3), the background corrected centromeric pixel intensities for EGFP-CID and EYFP-CENP-C were determined as outlined above. The pixel intensities determined for the frame immediately before bleaching were normalized to one, and during recovery, the cumulative pixel intensities for all bleached centromeres were plotted. In the "regional" FRAP experiments (Fig. S3) approximately 8 nuclei for each cell cycle stage were bleached within a larger optical field and initial recovery of fluorescence at the centromeres was monitored. For background correction, the values of cytoplasmic pixels within the bleached regions were used. When only single metaphase plates were bleached within a very small R.O.I. (Fig. 2), the entire cytoplasmic region was used for determination of background pixel values. Data from three independent experiments were combined for the plots. For the plot shown in Fig. 2B only series were aligned in which bleaching took place two frames (app. 14 sec) before the metaphase-to-anaphase transition.

For the determination of single centromere intensities of EGFP-CID (Fig. 1B), in each frame every centromere that was in focus and not tightly clustered with other centromeres, was selected with a circular R.O.I. slightly larger than the centromere itself. The mean pixel intensity was calculated and background correction was performed by subtracting mean cytoplasmic fluorescence intensities determined as for the nuclear EGFP-CID fluorescence intensity evaluation (see above). Three independent time series were aligned using the metaphase-to-anaphase transition as reference point, normalized to the first displayed time point in interphase, and mean values for the series were calculated and plotted as intensity per

centromere. Each data point represents the average intensity determined for a total of 50 to 200 individual centromeres. With the beginning of metaphase, the separate evaluation of sister centromeres results in an approximate 50% drop of the intensity per centromere. In late anaphase and telophase, the evaluation of single centromeres was impossible due to clustering of the signals resulting in a gap between the data points III and IV of Fig. 1B. For a false color illustration, the lookup table “Fire” available with the ImageJ software was employed. The point-like signals of tetR-EGFP fusion proteins (Fig. S2) were evaluated in an identical fashion as the single centromeres.

For the evaluation of EGFP-CID signal intensities in a *cid* mutant background (Fig. S1), the segmentation algorithm could not be applied since no His2Av-mRFP1 was present. Instead, centromere groups that were in focus were selected manually and mean pixel intensities were calculated. For background correction, the mean pixel intensities of manually selected cytoplasmic regions were subtracted, which were determined for each frame.

For the quantitation of EGFP-CID fluorescence intensity during the postblastoderm mitoses 15 and 16, time resolved z-stacks using the Leica DM-IRBE/TCS SP1 confocal system were recorded. In these later cycles the cells do not divide synchronously in the same plane and the daughter nuclei often move perpendicular to the surface during cell division. Three slices, 0.7 µm apart, were recorded in 20 sec intervals. Identification of centromere groups by segmentation and background correction were performed for every slice as described above. R.O.I.s were defined and evaluated for metaphase and for anaphase figures in every slice. Only the highest of the three metaphase values and the highest of the six daughter anaphase values within the three z-slices for one dividing cell were used for calculating the mean fluorescence intensities. For comparison, the same recording and evaluation procedure was also used to measure fluorescence intensities during syncytial

divisions. As a control for bleaching effects, an equal number of images were taken from a stage 11 embryo at short succession under identical conditions. The evaluation of the total fluorescence intensity revealed no significant reduction due to bleaching (<1%).

Aphidicolin (295 µM in 1% (v/v) DMSO) and colcemid (1 mM in 10% (v/v) DMSO) were injected laterally into the embryos. Time lapse recordings started immediately after the injections. As no anaphase resulting in separation of the sister centromeres occurred after colcemid injection, intensities were determined for the total centromere-localized fluorescence per nucleus throughout the experiment.

Supplemental Figure Legends

Fig. S1. Incorporation of EGFP-CID during anaphase in a *cid* mutant background. Living embryos expressing exclusively *EGFP-cid* in a transheterozygous *cid* mutant background (line $cid^{T12\text{-}1}/cid^{T22\text{-}4}$; *EGFP-cid* III.2/*EGFP-cid* III.2) were observed while progressing through mitosis 11. Images were acquired in 10 second intervals. The fluorescence intensity of EGFP-CID in a total of fourteen selected nuclei was determined for each frame. Data sets from two embryos were aligned using the first frame indicating the onset of anaphase (labeled II). The fluorescence intensities of interphase nuclei were normalized to 100% at the start of image acquisition. The graph represents the average values obtained in the two experiments. The gray line in the graph indicates the calculated fluorescence intensities of individual sister centromere groups per nucleus before their actual evaluation is possible, obtained by halving the measured intensities at these time points. (B), Images corresponding to selected time points (indicated by arrows numbered with roman numerals in (A)) of one of the series. The pixel values have been reversed for clarity. Arrows indicate groups of centromeric signals belonging together. The actual frames used for data evaluation were 4 times the area of the frames illustrated in the figure. The enlargements are shown for clarity. One mitotic figure has been enlarged even further and the increase in pixel intensity during anaphase is illustrated using a false color representation (B, middle panel). The same mitotic figure is shown in a binary representation in the bottom panel with only those pixels displayed that have a value above 70. The actual pixel numbers are given in the lower left corners. The increase during anaphase of the number of pixels above the threshold of 70 is obvious.

Fig. S2. The fluorescence intensity of tetR-EGFP fusion proteins bound to chromosomally integrated *tet*-operator arrays does not increase during anaphase. Living embryos expressing *tetR-EGFP* and containing chromosomally integrated *tet*-operator-repeats were observed while progressing through mitosis 12 or 13 (A). Images were acquired every 19 s. Single tetR-EGFP dots were selected and the background corrected intensities were determined. (B), Intensities are plotted per tetR-EGFP dot. The graph represents data obtained from 4 embryos. For the five time points (145 s) after the metaphase-to-anaphase transition, which is the time frame when CID and CENP-C incorporation occurs, a total of 22 to 39 focused fluorescent dots were evaluated per time point. The fluorescence intensity of tetR-EGFP stays low after the metaphase-to-anaphase transition. Red arrows indicate the time points from which the sample images shown in (A) were taken. Data are presented as mean +/- SD.

Fig. S3. EGFP-CID and EYFP-CENP-C are most dynamic during anaphase. Living embryos expressing *His2Av-mRFP1* and *EGFP-cid* or *EYFP-Cenp-C* were observed while progressing through mitosis 12. During various cell cycle stages, R.O.I.s were selected and bleached with high laser power at 488 nm. The recovery of centromeric EGFP-CID and EYFP-CENP-C fluorescence was monitored. (A) Example of a time lapse series after bleaching of multiple mitotic figures during anaphase used for quantitation. EGFP-CID fluorescence is shown in dark green. The contours of the DNA masses of the dividing nuclei are indicated by fine gray lines. Initial FRAP dynamics for EGFP-CID (B) and EYFP-CENP-C (C) after bleaching were monitored. Data sets from three to four independent experiments were combined. The fluorescence intensity after bleaching was set to zero. Error bars indicate standard deviations. Only little recovery was obtained when EGFP-CID and EYFP-CENP-C were bleached during interphase suggesting that both proteins are stably associated with the centromeres at this stage (B, C, blue curves). The slight recovery of fluorescence may be due to reversible

photobleaching of GFP variants [S14]. Increased recovery rates of fluorescence were observed during mitosis. Quantitation during metaphase (B, C, pink curves) revealed that recovery rates were approximately three times as high as during interphase suggesting increased turnover of both CID and CENP-C, as no considerable net incorporation was recorded during this phase. Significantly, highest recovery rates were recorded during anaphase (B, C, red curves). The initial rates do not support a full recovery during anaphase in contrast to the measurements using single bleached mitotic figures (Fig. 2B), most probably because in the "regional" bleaching experiments a significant fraction of bleached molecules derived from the larger bleached cytoplasmic pool surrounding the chromatin becomes incorporated. We could not perform half-life determinations because a recovery to saturation could not be obtained due to the short duration of anaphase of about only 90 seconds. Thus, the graphs in (B) and (C) represent the initial, approximately linear course of recovery rather than the exponential recovery curves typical for FRAP experiments. Data are presented as mean +/- SD.

Fig. S4. The fluorescence intensity of His2Av-mRFP1 does not change during mitosis when colcemid is injected in spindle checkpoint deficient embryos or when DNA replication is inhibited. Living embryos expressing *His2Av-mRFP1* and *EGFP-cid* were observed while progressing through syncytial mitoses, and His2Av-mRFP1 fluorescence intensity was quantitated and plotted as in Fig. 1D. Colcemid (A) or aphidicolin (B) were injected to inhibit spindle formation or DNA replication, respectively. Injected embryos were wild type (B) or devoid of a functional spindle checkpoint due to the lack of the checkpoint kinase Mps1 (A). The gray lines in (A) and (B) indicate the fluorescence intensity changes of EGFP-CID as shown in Fig. 3A ($Mps1^{-/-}$) and Fig. 3B, respectively. The graphs represent average values obtained from 4 to 5 embryos. Data for His2Av-mRFP1 are presented as mean +/- SD.

Fig. S5. EGFP-CID is not incorporated into centromeres during the postblastoderm mitoses 15 and 16. Living embryos expressing *EGFP-cid* and *His2Av-mRFP1* were observed while progressing through epidermal mitosis 15 (A), 16 (B) and the syncytial mitoses 12 or 13 (C). Z-stacks (3 planes, 0.7 µm apart) were recorded every 20 sec. Fluorescence intensities of EGFP-CID were determined for selected nuclei in each image. Only the highest value for a certain nucleus obtained from one of the three planes within a z-stack was used to calculate the intensity at a specific time point. The mean intensities of centromeric EGFP-CID fluorescence are plotted as relative intensities per nucleus. Beginning at the onset of anaphase (red arrows), segregating sister centromere groups were evaluated separately, resulting in an approximately 50% intensity drop. Data sets from three embryos were combined. While the fluorescent intensities after progressing through mitoses 15 and 16 remained at the level of approximately 50% for at least 5 min (A, B) , it increased rapidly when nuclei in syncytial embryos were observed using the same conditions (C). Data are presented as mean +/- SD.

Movie S1. Mitosis 12 of a syncytial embryo expressing EGFP-CID (green) and His2Av-mRFP1 (red). Single confocal planes were recorded every 24 s. Shown is a representative movie of many independent experiments.

Movie S2. FRAP analysis of EGFP-cid. Embryos expressing HisAv-mRFP1 (red) and EGFP-cid (green) were monitored. A single metaphase plate of an embryo progressing through mitosis 12 was selected and bleached with 4 iterations of the 488 nm laser at 100% power. Single confocal planes were recorded every 11.5 s. The recovery of EGFP-CID fluorescence

during anaphase is obvious. Shown is a representative movie of many independent experiments.

Supplementary References

S1. Kalitsis, P., Fowler, K.J., Earle, E., Griffiths, B., Howman, E., Newson, A.J., and Choo, K.H. (2003). Partially functional Cenpa-GFP fusion protein causes increased chromosome missegregation and apoptosis during mouse embryogenesis. Chromosome Res. *11*, 345-357.

S2. Malik, H.S., Vermaak, D., and Henikoff, S. (2002). Recurrent evolution of DNA-binding motifs in the Drosophila centromeric histone. Proc. Natl. Acad. Sci. USA *99*, 1449-1454.

S3. Horn, C., and Wimmer, E.A. (2000). A versatile vector set for animal transgenesis. Dev. Genes Evol. *210*, 630-637.

S4. Pirrotta, V. (1988). Vectors for P-element transformation in Drosophila. In Vectors A survey of cloning vectors and their uses, R.L. Rodriguez and D.T. Denhardt, eds. (Boston and London: Butterworths), pp. 437-456.

S5. Campbell, R.E., Tour, O., Palmer, A.E., Steinbach, P.A., Baird, G.S., Zacharias, D.A., and Tsien, R.Y. (2002). A monomeric red fluorescent protein. Proc. Natl. Acad. Sci. USA *99*, 7877-7882.

S6. Clarkson, M., and Saint, R. (1999). A His2AvDGFP fusion gene complements a lethal His2AvD mutant allele and provides an in vivo marker for Drosophila chromosome behavior. DNA Cell Biol. *18*, 457-462.

S7. Michaelis, C., Ciosk, R., and Nasmyth, K. (1997). Cohesins: Chromosomal proteins that prevent premature separation of sister chromatids. Cell *91*, 35-45.

S8. Tracey, W.D., Jr., Ning, X., Klingler, M., Kramer, S.G., and Gergen, J.P. (2000). Quantitative analysis of gene function in the Drosophila embryo. Genetics *154*, 273-284.

S9. Blower, M.D., Daigle, T., Kaufman, T., and Karpen, G.H. (2006). Drosophila CENP-A mutations cause a BubR1-dependent early mitotic delay without normal localization of kinetochore components. PLoS Genet. *2*, e110.

S10. Heeger, S., Leismann, O., Schittenhelm, R., Schraidt, O., Heidmann, S., and Lehner, C.F. (2005). Genetic interactions of separase regulatory subunits reveal the diverged Drosophila Cenp-C homolog. Genes Dev. *19*, 2041-2053.

S11. Fischer, M.G., Heeger, S., Häcker, U., and Lehner, C.F. (2004). The mitotic arrest in response to hypoxia and of polar bodies during early embryogenesis requires Drosophila Mps1. Curr. Biol. *14*, 2019-2024.

S12. Pandey, R., Heidmann, S., and Lehner, C.F. (2005). Epithelial re-organization and dynamics of progression through mitosis in Drosophila separase complex mutants. J. Cell Sci. *118*, 733-742.

S13. Black, M.J., Sapiro, G., Marimont, D.H., and Heeger, D. (1998). Robust anisotropic diffusion. IEEE Transactions on Image Processing *7*, 421-432.

S14. Sinnecker, D., Voigt, P., Hellwig, N., and Schaefer, M. (2005). Reversible photobleaching of enhanced green fluorescent proteins. Biochemistry *44*, 7085-7094.

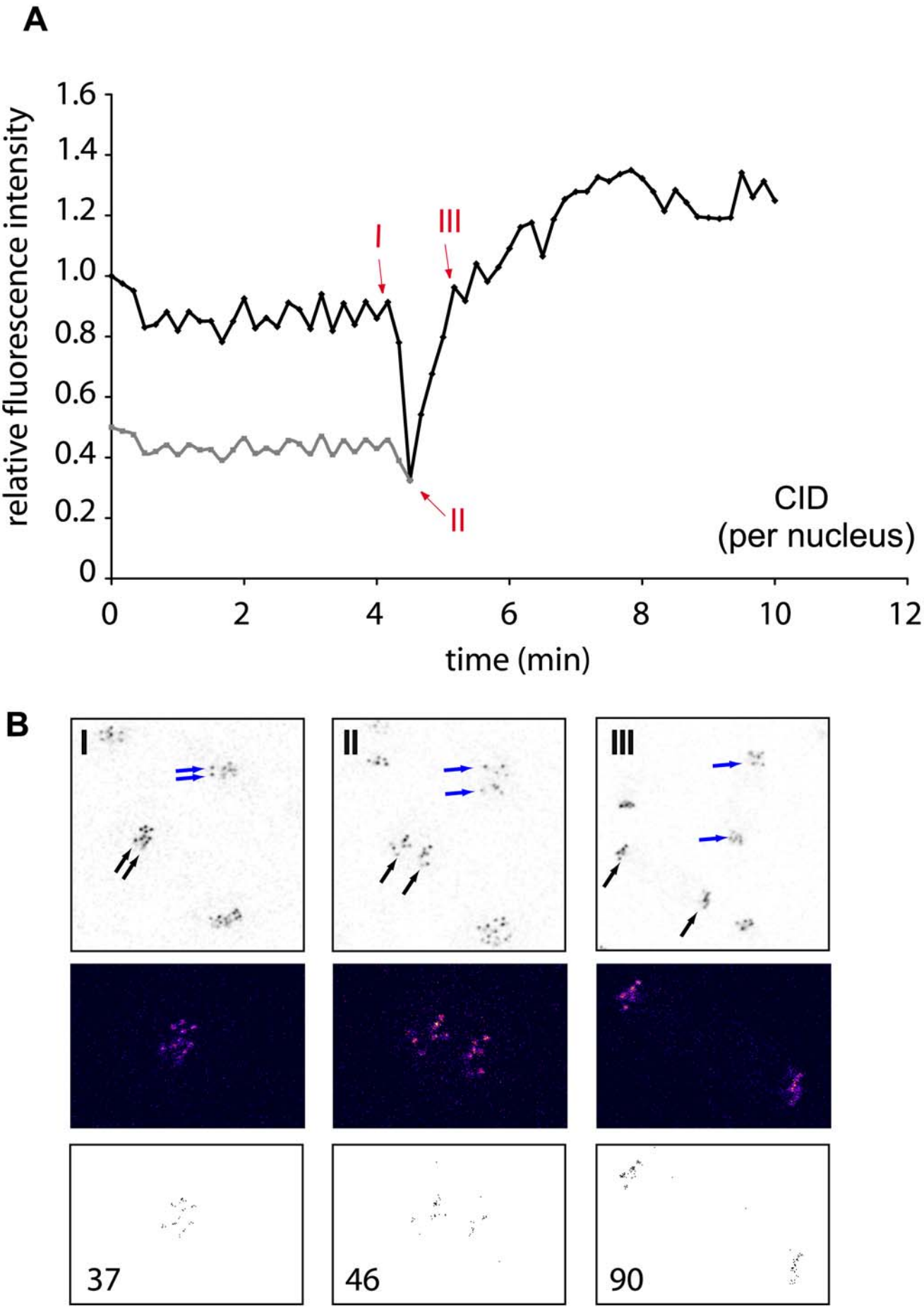
A
relative fluorescence intensity
1.6
1.4
1.2
1.0
0.8
0.6
0.4
0.2
0
I
III
II
CID
(per nucleus)
0
2
4
6
8
10
12
time (min)
B
I
II
III
37
46
90

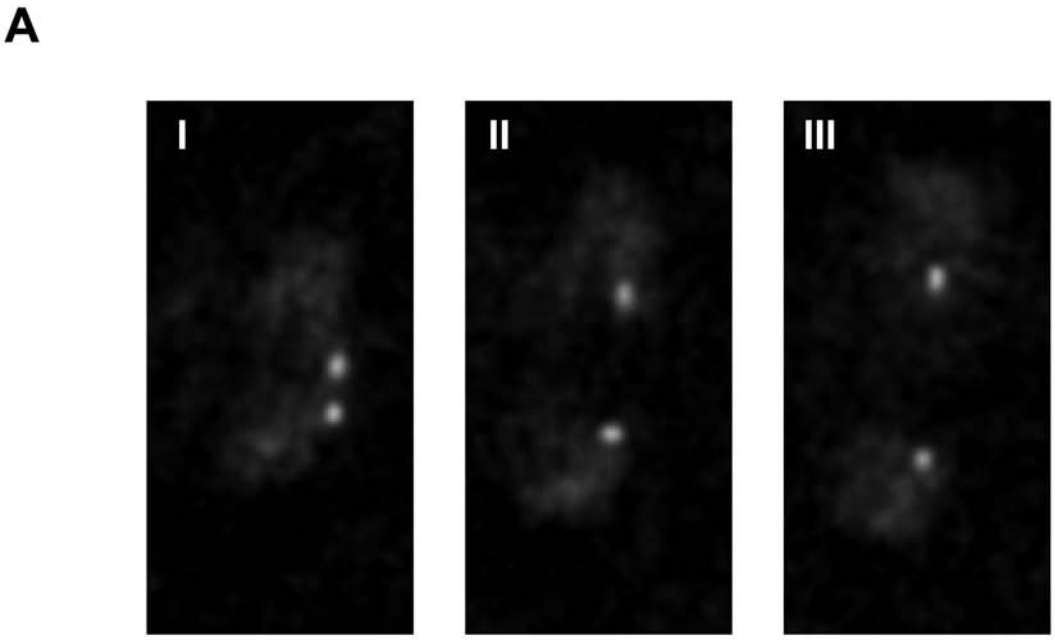
A
I
II
III
B
relative fluorescence intensity
1.6
1.4
1.2
1.0
0.8
0.6
0.4
0.2
0
tetR-EGFP
(per nucleus)
I
II
III
0
1
2
3
4
5
6
7
time (min)

Schuh et al, Supplementary Figure 3

A

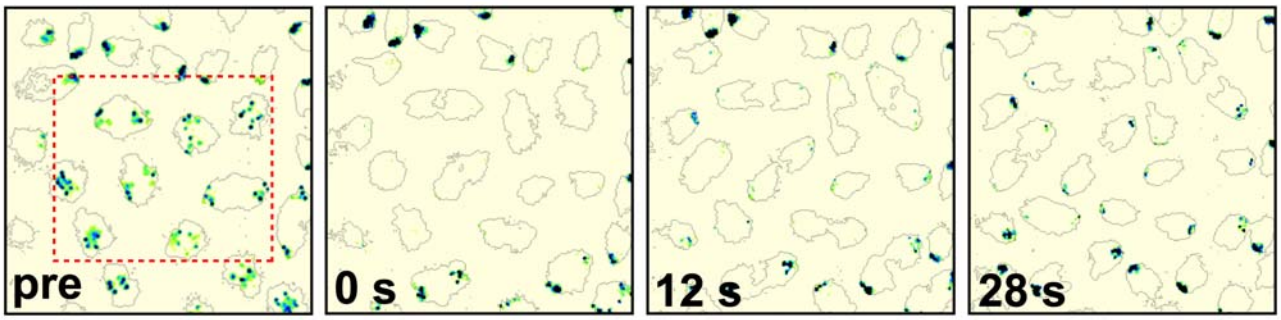

B

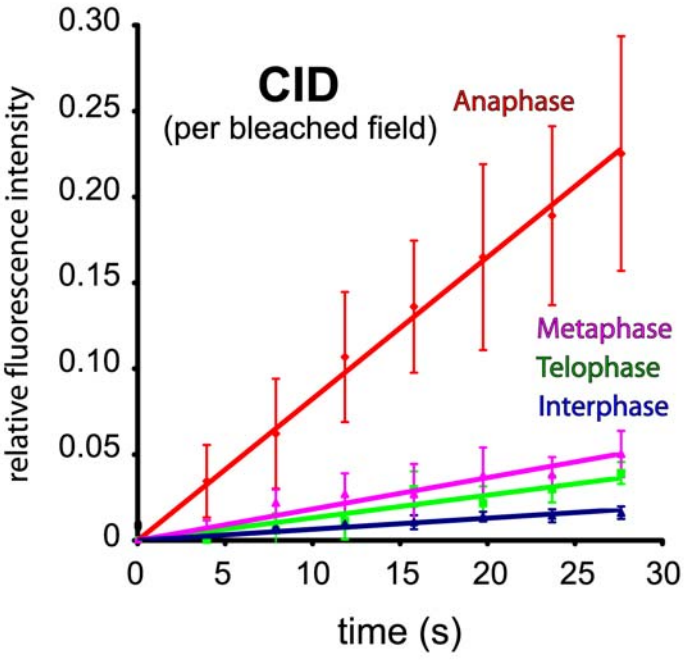

C

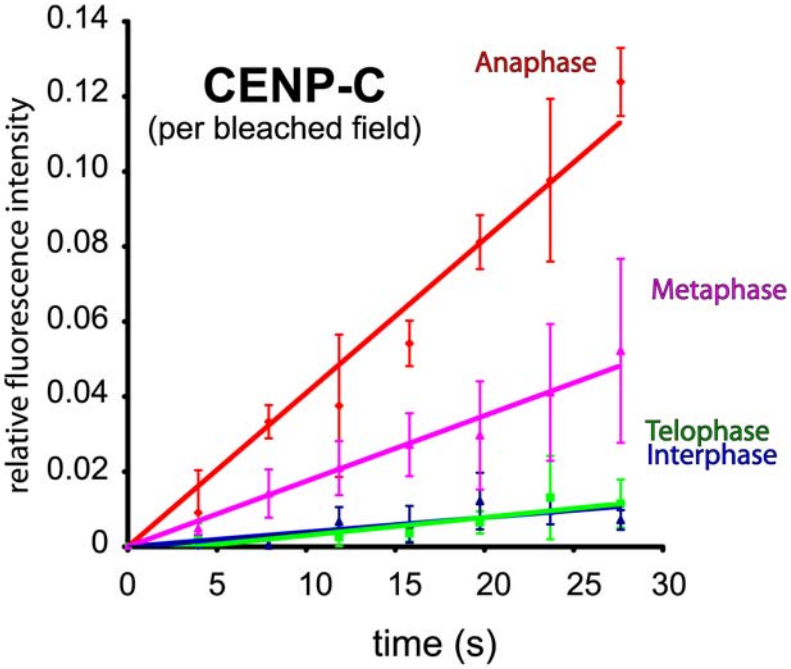

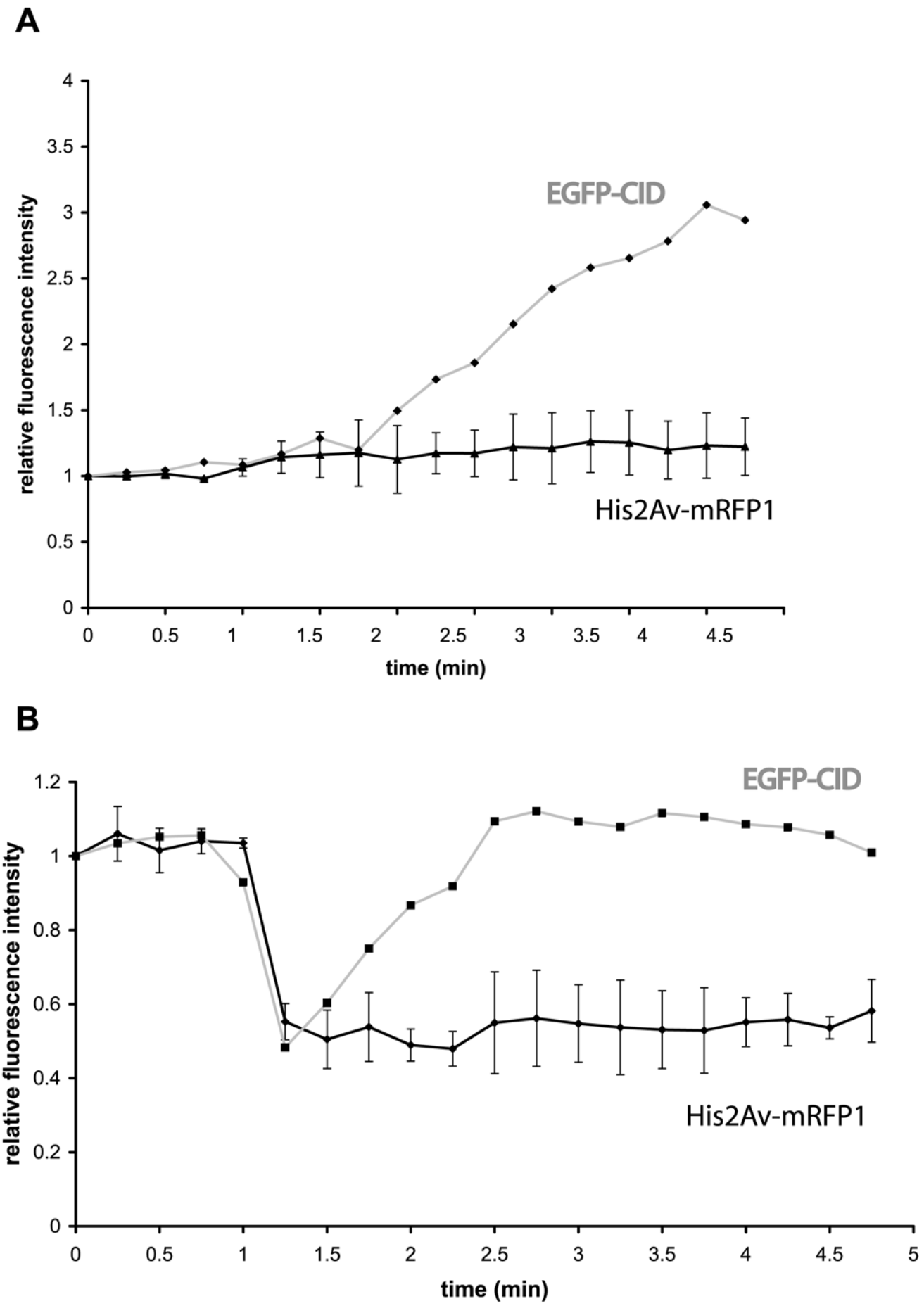
A
relative fluorescence intensity
time (min)
EGFP-CID
His2Av-mRFP1
B
relative fluorescence intensity
time (min)
EGFP-CID
His2Av-mRFP1

Schuh et al, Supplementary Figure 5